Planar Vibrations of LIBRA INPORT Tubes Including Gravity Gradient Effects

R.L. Engelstad and E.G. Lovell

October 1984

FPA-84-3

FUSION POWER ASSOCIATES

2 Professional Drive, Suite 248
Gaithersburg, Maryland 20879
(301) 258-0545

1500 Engineering Drive
Madison, Wisconsin 53706
(608) 263-2308

PLANAR VIBRATIONS OF LIBRA INPORT TUBES INCLUDING GRAVITY GRADIENT EFFECTS

R.L. Engelstad

E.G. Lovell

Fusion Power Associates
6515 Grand Teton Plaza
Room 245
Madison, Wisconsin 53719

October 1984

FPA-84-3

I. INTRODUCTION

Key design considerations for the LIBRA cavity depend upon the mechanical response of INPORTs under repetitive shock loading. The determination of the response requires the quantitative characteristics for mode shapes and natural frequencies. Since the axial tension gradient is significant for INPORTs, this will affect the modal analysis. In the work which follows, the tension gradient is assessed in the development of an exact solution for INPORT mode shapes and natural frequencies.

II. NOMENCLATURE

a_m - perturbation parameter

A_f - cross sectional flow area

A_t - cross section of tube

b_n - perturbation parameter

c - flow velocity

E - elastic modulus of tube

g - gravitational constant

I - moment of inertia of tube section

ℓ - tube length

m - integer

m_f - mass/length of fluid

m_t - mass/length of tube

M - total mass/length ($m_f + m_t$)

n - integer

p - internal mean pressure

t - time

T_e - effective tension

T_o - static pretension

$\overline{T}$ - dimensionless tension

u - x displacement

v - y displacement

V_n - modal amplitude

w - z displacement

W - total weight of tube and fluid

x - axial coordinate

y - transverse coordinate

z - transverse coordinate

δ - perturbation function

ε - perturbation function

κ_o - damping coefficient

ν - Poisson's ratio for tube

ω_n - natural frequency

$\overline{\omega}_n$ - dimensionless natural frequency

III. GOVERNING EQUATION

The system under consideration (Fig. 1) consists of a uniform tube of length ℓ, cross sectional flow area A_f, mass per unit length m_t, and flexural rigidity EI. The internal fluid flows axially with velocity c and mass per unit length m_f. Any secondary flow effects or radial variations in the flow velocity are neglected. The mean pressure within the tube is p, measured above atmospheric. However, it is assumed that the nominal dimensions of the tube will not change with the internal pressure.

In its undeformed (equilibrium) position the longitudinal axis of the tube coincides with the x axis. With this vertical configuration, gravity ef-

fects will be assessed. Free and forced response of the tube is allowed in both the x-y and x-z planes along with longitudinal deformations.

With a compression spring mechanism supporting both ends, a static pretension T_o can be applied to the system. An additional axial tensile force is induced by the internal pressure, which is equal to $pA_f(2\nu - 1)$ for a thin tube. Nonlinear tension effects can be included by considering higher order terms in the expression for the tube extension. Also, since the weight of the viscid fluid is not negligible, there will be a tension variation due to a gravity gradient.

The general equations of motion for the tube were derived using Hamilton's principle and variational calculus procedures.[1] The resulting partial differential equation for lateral motion in the x-y plane is given by

$$
\begin{aligned}
&(m_f + m_t)\frac{\partial^2 v}{\partial t^2} + 2\, m_f c \frac{\partial^2 v}{\partial x \partial t} + m_f c^2 \frac{\partial^2 v}{\partial x^2} + \kappa_o m_t \frac{\partial v}{\partial t} - \frac{\partial}{\partial x}\{[T_o - pA_f(1 - 2\nu) \\
&\quad + (m_f + m_t)g(\ell - x)] + [EA_t - T_o - pA_f(1 - 2\nu) - (m_f + m_t)g(\ell - x)] \\
&\quad \times [\frac{\partial u}{\partial x} - (\frac{\partial u}{\partial x})^2 + \frac{1}{2}(\frac{\partial v}{\partial x})^2 + \frac{1}{2}(\frac{\partial w}{\partial x})^2]\frac{\partial v}{\partial x}\} + EI\frac{\partial^4 v}{\partial x^4} - 3\, EI\,(\frac{\partial v}{\partial x})^2 \frac{\partial^4 v}{\partial x^4} \\
&\quad -12\, EI \frac{\partial v}{\partial x}\frac{\partial^2 v}{\partial x^2}\frac{\partial^3 v}{\partial x^3} - 3\, EI\,(\frac{\partial^2 v}{\partial x^2})^3 = 0
\end{aligned}
\tag{1}
$$

where steady state flow has been assumed.

In order to determine the basic modal characteristics of the tube, Eq. (1) has been linearized to decouple the lateral and longitudinal displacements. For transverse motion it is assumed that the effect of the Coriolis acceleration of the fluid, given by $2m_f c(\partial^2 v/\partial x \partial t)$, can be neglected. Also, since the INPORTs are considered as completely flexible tubes, Eq. (1) becomes

$$[T_o - pA_f(1 - 2\nu) + (m_t + m_f)g(\ell - x) - m_f c^2] \frac{\partial^2 v}{\partial x^2} - (m_t + m_f)\, g \frac{\partial v}{\partial x}$$

$$- \kappa_o (m_t + m_f) \frac{\partial v}{\partial t} - (m_t + m_f) \frac{\partial^2 v}{\partial t^2} = 0 \qquad (2)$$

or,

$$\frac{\partial}{\partial x} \{[(T_o - pA_f(1 - 2\nu) + (m_t + m_f)g(\ell - x) - m_f c^2] \frac{\partial v}{\partial x}\}$$

$$- \kappa_o (m_t + m_f) \frac{\partial v}{\partial t} - (m_t + m_f) \frac{\partial^2 v}{\partial t^2} = 0 \; . \qquad (3)$$

The equation of motion may be expressed in dimensionless terms by defining the following dimensionless quantities:

$$\bar{v} = \frac{v}{\ell}$$

$$\xi = \frac{T_o - pA_f(1 - 2\nu) + (m_t + m_f)g(\ell - x) - m_f c^2}{(m_t + m_f)g\ell} \qquad (4)$$

$$\tau = \sqrt{\frac{g}{\ell}}\, t \; .$$

Substitution into Eq. (3) yields

$$\frac{\partial}{\partial \xi} \{\xi \frac{\partial \bar{v}}{\partial \xi}\} - \kappa \frac{\partial \bar{v}}{\partial \tau} - \frac{\partial^2 \bar{v}}{\partial \tau^2} = 0 \qquad (5)$$

where the damping parameter κ is given by

$$\kappa = \kappa_o \sqrt{\frac{\ell}{g}} \; . \qquad (6)$$

Equation (5) can be reduced to an ordinary differential equation by assuming a harmonic solution of the form

$$\bar{v}(\xi,\tau) = \mathrm{Re}\{\phi(\xi)\bar{X}e^{i\bar{\omega}\tau}\} \tag{7}$$

where $\phi(\xi)$ is a complex function and $\bar{\omega}$ is the dimensionless frequency. Substitution of Eq. (7) into (5) gives

$$\frac{d}{d\xi}\left(\xi\,\frac{d\phi(\xi)}{d\xi}\right) + (\bar{\omega}^2 - i\kappa\bar{\omega})\,\phi(\xi) = 0\ . \tag{8}$$

The solution to Eq. (8) involves Bessel functions of the first and second kind of zero order,[2] namely

$$\phi(\xi) = AJ_0(\lambda\sqrt{\xi}) + BY_0(\lambda\sqrt{\xi}) \tag{9}$$

where

$$\lambda = \{4(\bar{\omega}^2 - i\kappa\bar{\omega})\}^{1/2}\ . \tag{10}$$

For a general solution A and B must be complex constants.

A closer look at the argument of J_0 and Y_0 indicates

$$\lambda\sqrt{\xi} = \{4\bar{\omega}^2(\bar{T} - \tfrac{x}{\ell}) - 4i\kappa\bar{\omega}(\bar{T} - \tfrac{x}{\ell})\}^{1/2} \tag{11}$$

where the dimensionless tension and frequency are given by

$$\bar{T} = \frac{T_o - pA_f(1 - 2\nu) + (m_t + m_f)g\ell - m_f c^2}{(m_t + m_f)g\ell} \tag{12}$$

$$\bar{\omega} = \sqrt{\frac{\ell}{g}}\,\omega \ . \tag{13}$$

Finally, the complete solution to Eq. (5) can be expressed as a superposition of an infinite set of the normal modes of the tube, i.e.,

$$\bar{v}(\xi,\tau) = \mathrm{Re}\Big\{ \sum_{n=1}^{\infty} \phi_n(\xi)\bar{X}_n e^{i\bar{\omega}_n \tau} \Big\} \tag{14}$$

which also includes the complex constant

$$\bar{X}_n = X_n e^{i\alpha_n} \tag{15}$$

where X_n and α_n are determined by initial conditions. Here $\phi_n(\xi)$ represents the eigenfunctions of the tube which must satisfy the boundary conditions of the problem. For this case

$$\bar{v}(\xi,\tau) = \phi_n(\xi) = 0 \qquad \text{at } x = 0 \text{ and } x = \ell \ . \tag{16}$$

Equation (16) can then be used to determine the dimensionless frequencies $\bar{\omega}_n$ and complex constants A_n and B_n of Eq. (9).

For convenience, Eq. (14) has been rewritten so it contains only the real part. Complex terms can be broken up into their real and imaginary parts by letting

$$A_n = A_{Rn} + iA_{In}$$

$$B_n = B_{Rn} + iB_{In}$$

$$J_o(\lambda_n\sqrt{\xi}) = J_{oR}(\lambda_n\sqrt{\xi}) + iJ_{oI}(\lambda_n\sqrt{\xi}) \tag{17}$$

$$Y_o(\lambda_n\sqrt{\xi}) = Y_{oR}(\lambda_n\sqrt{\xi}) + iY_{oI}(\lambda_n\sqrt{\xi})$$

where R and I represent the real and imaginary parts, respectively. Also, let

$$\bar{X}_n e^{i\bar{\omega}_n\tau} = X_n e^{i(\bar{\omega}_n\tau - \alpha_n)} . \tag{18}$$

Equations (17) and (18) are substituted into (9) and (14). After simplifying and retaining the real part only

$$\bar{v}(\xi,\tau) = \sum_{n=1}^{\infty} X_n[A_{Rn}J_{oR}(\lambda_n\sqrt{\xi}) - A_{In}J_{oI}(\lambda_n\sqrt{\xi}) + B_{Rn}Y_{oR}(\lambda_n\sqrt{\xi}) - B_{In}Y_{oI}(\lambda_n\sqrt{\xi})]$$

$$\times \cos(\bar{\omega}_n\tau - \alpha_n) - X_n[A_{Rn}J_{oI}(\lambda_n\sqrt{\xi}) + A_{In}J_{oR}(\lambda_n\sqrt{\xi}) + B_{Rn}Y_{oI}(\lambda_n\sqrt{\xi})$$

$$+ B_{In}Y_{oR}(\lambda_n\sqrt{\xi})] \times \sin(\bar{\omega}_n\tau - \alpha_n) \tag{19}$$

which is the general solution to Eq. (5).

To determine natural frequencies and mode shapes, the eigenfunctions $\phi_n(\xi)$ are required to satisfy the boundary conditions given in Eq. (16). This results in the following set of equations

$$A_{Rn}J_{oR}(\lambda_n\sqrt{\xi_1}) - A_{In}J_{oI}(\lambda_n\sqrt{\xi_1}) + B_{Rn}Y_{oR}(\lambda_n\sqrt{\xi_1}) - B_{In}Y_{oI}(\lambda_n\sqrt{\xi_1}) = 0$$

$$A_{Rn}J_{oI}(\lambda_n\sqrt{\xi_1}) + A_{In}J_{oR}(\lambda_n\sqrt{\xi_1}) + B_{Rn}Y_{oI}(\lambda_n\sqrt{\xi_1}) + B_{In}Y_{oR}(\lambda_n\sqrt{\xi_1}) = 0$$

$$A_{Rn}J_{oR}(\lambda_n\sqrt{\xi_2}) - A_{In}J_{oI}(\lambda_n\sqrt{\xi_2}) + B_{Rn}Y_{oR}(\lambda_n\sqrt{\xi_2}) - B_{In}Y_{oI}(\lambda_n\sqrt{\xi_2}) = 0 \qquad (20)$$

$$A_{Rn}J_{oI}(\lambda_n\sqrt{\xi_2}) + A_{In}J_{oR}(\lambda_n\sqrt{\xi_2}) + B_{Rn}Y_{oI}(\lambda_n\sqrt{\xi_2}) + B_{In}Y_{oR}(\lambda_n\sqrt{\xi_2}) = 0$$

where ξ_1 and ξ_2 have been used to represent ξ evaluated at $x = 0$ and $x = \ell$, respectively. For a nontrivial solution to (20) the n determinants of the terms multiplying the A's and B's must equal zero, i.e.,

$$\begin{vmatrix} J_{oR}(\lambda_n\sqrt{\xi_1}) & -J_{oI}(\lambda_n\sqrt{\xi_1}) & Y_{oR}(\lambda_n\sqrt{\xi_1}) & -Y_{oI}(\lambda_n\sqrt{\xi_1}) \\ J_{oI}(\lambda_n\sqrt{\xi_1}) & J_{oR}(\lambda_n\sqrt{\xi_1}) & Y_{oI}(\lambda_n\sqrt{\xi_1}) & Y_{oR}(\lambda_n\sqrt{\xi_1}) \\ J_{oR}(\lambda_n\sqrt{\xi_2}) & -J_{oI}(\lambda_n\sqrt{\xi_2}) & Y_{oR}(\lambda_n\sqrt{\xi_2}) & -Y_{oI}(\lambda_n\sqrt{\xi_2}) \\ J_{oI}(\lambda_n\sqrt{\xi_2}) & J_{oR}(\lambda_n\sqrt{\xi_2}) & Y_{oI}(\lambda_n\sqrt{\xi_2}) & Y_{oR}(\lambda_n\sqrt{\xi_2}) \end{vmatrix} = 0 \quad n = 1,2,3,\ldots,\infty \qquad (21)$$

The solution procedure, then, involves choosing a value of $\bar{\omega}$, calculating the argument given by Eq. (11) and corresponding Bessel function, and finally checking the value of the determinant. After $\bar{\omega}$ is found, the relative values of the complex constants A and B can be determined from (21). This procedure is repeated until the number of modes identified is sufficient to completely describe the tube motion.

IV. NUMERICAL RESULTS

An analysis was performed to determine natural frequencies and mode shapes for the special case of zero damping. Setting the damping parameter,

κ, to zero in Eq. (11), eliminates the imaginary term of the argument. With the restriction $\overline{T} > 1.0$, J_o and Y_o are assured to be real. Consequently, the equations in (20) will uncouple giving the following two sets of equations

$$\begin{aligned} A_{Rn}J_{oR}(\lambda_n\sqrt{\xi_1}) + B_{Rn}Y_{oR}(\lambda_n\sqrt{\xi_1}) &= 0 \\ A_{Rn}J_{oR}(\lambda_n\sqrt{\xi_2}) + B_{Rn}Y_{oR}(\lambda_n\sqrt{\xi_2}) &= 0 \end{aligned} \tag{22}$$

$$\begin{aligned} A_{In}J_{oR}(\lambda_n\sqrt{\xi_1}) + B_{In}Y_{oR}(\lambda_n\sqrt{\xi_1}) &= 0 \\ A_{In}J_{oR}(\lambda_n\sqrt{\xi_2}) + B_{In}Y_{oR}(\lambda_n\sqrt{\xi_2}) &= 0 \ . \end{aligned}$$

From the above, it is obvious that

$$\begin{aligned} A_{Rn} &= A_{In} \\ B_{Rn} &= B_{In} \end{aligned} \tag{23}$$

and the necessary condition for a nontrivial solution is

$$J_{oR}(\lambda_n\sqrt{\xi_1})Y_{oR}(\lambda_n\sqrt{\xi_2}) - Y_{oR}(\lambda_n\sqrt{\xi_1})J_{oR}(\lambda_n\sqrt{\xi_2}) = 0 \ . \tag{24}$$

Therefore, Eq. (24) is used to define the natural frequencies of the system.

Along the same lines, the eigenfunctions describing the mode shapes can be simplified to:

$$\phi_n(\xi) = C_n\left[J_o(\lambda_n\sqrt{\xi}) - \frac{J_o(\lambda_n\sqrt{\xi_1})}{Y_o(\lambda_n\sqrt{\xi_1})}\,Y_o(\lambda_n\sqrt{\xi})\right] \tag{25}$$

where C_n is an arbitrary constant and can be incorporated into X_n in (18).

Equations (24) and (25) have been programmed to cover a range of tensions, $\overline{T}$. Accuracy problems arise when solving these equations since the arguments of the Bessel functions given in (11) can become "relatively" large. Therefore, to eliminate the possibility of round-off errors, calculations were done on a Cray computer. Function subroutines from IMSL were used to calculate J_0's and Y_0's. These allowed arguments in the following ranges

Function	Range of Argument
J_0	$<< 1.3 \times 10^8$
Y_0	2.9×10^{-39} to 1.3×10^8

where both single and double precision are supported. Also, the method of bisection, based on the use of sign changes to detect a zero, was used to determine the roots of (24).

The first ten natural frequencies computed are shown in Fig. 2. Tabular values to three decimal places corresponding to these curves are given in Table 1. Calculations were performed letting $\overline{T}$ approach 1 since $Y_0(0)$ is negatively infinite. Figures 3-12 show the first ten mode shapes for dimensionless tensions of 1.1, 2.0 and 3.0. Again Tables 2-4 show the tabulated values of these mode shapes. For convenience, each has been individually normalized. Asymmetry is considerably noticeable with the lower tensions. Figure 13 shows the shifts of the maximum amplitude and zero crossing for modes 1 and 2 due to the nonlinear effects of the tension. Consequently, as $\overline{T}$ becomes much greater than the weight the natural frequencies and mode shapes will approach that of a classic string.

V. PERTURBATION ANALYSIS

In this section, a perturbation analysis is developed for the equation of motion of a completely flexible tube which has small gradients in axial tension and density. The purpose of the work is to provide a limited verification of the eigenvalue problem results previously obtained in exact form for the planar case with a linear tension gradient.

The relevant equation of motion (3) has been presented and is simply reproduced here in undamped form:

$$\frac{\partial}{\partial x}\left\{\left[T_o - pA_f(1 - 2\nu) + (m_t + m_f)g(\ell - x) - m_f c^2\right]\frac{\partial v}{\partial x}\right\} - (m_t + m_f)\frac{\partial^2 v}{\partial t^2} = 0 \ . \tag{26}$$

For small axial gradients, the following replacements are made for the effective tension and total mass per unit length

$$\left(T_o - pA_f(1 - 2\nu) - m_f c^2\right) \rightarrow T_e[1 + \delta(x)] \tag{27}$$

$$(m_t + m_f) \rightarrow M[1 + \varepsilon(x)] \ . \tag{28}$$

This problem is generalized slightly with $\delta(x)$ and $\varepsilon(x)$, but restricted by requiring both functions to have very small amplitudes.

The form of the solution used for a typical modal component can be expressed as

$$v_n(x,t) = \left[V_n(x) + \sum_{m \neq n} a_m V_m(x)\right] \exp(i\omega_n t) \tag{29}$$

$$\omega_n^2 = \omega_n^{*2}(1 + b_n) \ . \tag{30}$$

Here $V_n(x)$ and ω_n^* represent solutions to the gradient-free problem. The coefficients a_m and b_n are small order terms and facilitate the development of the perturbation solution. These equations can be substituted directly into (26)

$$\frac{\partial}{\partial x}\{[T_e(1 + \delta(x)][V_n' + \sum a_m V_m']\} + \omega_n^2 M[1 + \varepsilon(x)][V_n + \sum a_m V_m] = 0 \ . \tag{31}$$

This is now expanded

$$(T_e V_n'' + M\omega_n^{*2} V_n) + T_e \sum a_m V_m'' + T_e[\delta(x)V_n']' + M\omega_n^{*2} \sum a_m V_m + M\omega_n^{*2}[\varepsilon(x) + b_n]\, V_n \tag{32}$$

$$= -T_e[\sum \delta(x)\, a_m V_m']' - M\omega_n^{*2}[(1 + b_n)\varepsilon(x)] \sum a_m V_m \ .$$

If only first order perturbation terms are to be retained, quantities on the right side of (32) are neglected; the first pair of terms on the left side is identically zero. Thus

$$T_e[\delta(x)V_n']' + M\omega_n^{*2}[\varepsilon(x) + b_n]V_n + \sum_{m \neq n} a_m[T_e V_m'' + M\omega_n^{*2} V_m] = 0 \ . \tag{33}$$

The expression for determining the series coefficients, a_m, is obtained from (33) by taking the product with $V_p(x)$, $(p \neq n)$, and integrating over the length

$$a_m = \{T_e \int_0^{\ell} [\delta(x)V_n']'V_m \, dx + M\omega_n^{*2} \int_0^{\ell} \varepsilon(x) V_n V_m \, dx\}/k_m M(\omega_m^{*2} - \omega_n^{*2}) \tag{34}$$

where $V_m''(x) = -\omega_m^{*2} V_m(x) M/T_e$ and $k_m \int_0^{\ell} [V_m(x)]^2 \, dx$.

Using the same procedure, an expression for b_n can be developed by multiplying (33) by $V_n(x)$

$$b_n = -(T_e/Mk_n\omega_n^{*2}) \int_o^\ell [\delta(x)V_n']'V_n \, dx - (1/k_n) \int_o^\ell \varepsilon(x)V_n^2 \, dx \; . \tag{35}$$

When $\varepsilon(x)$ and $\delta(x)$ are specified, a_m and b_n can be calculated from (34) and (35).

The preceding analysis is now specialized for the problem in which the mass per unit length is constant and the tension varies linearly. The axial coordinate, x, originates as at the top with the positive direction downward, coincident with gravity as in Fig. 1:

$$M[1 + \varepsilon(x)] = M; \quad \varepsilon(x) = 0 \tag{36}$$

$$T_e[1 + \delta(x)] = T_e + W(1 - x/\ell) \; . \tag{37}$$

Here W denotes the total tube weight, assumed to be considerably less than the pretension T_e. The zero gradient mode shapes and frequencies are

$$V_n(x) = \sin n\pi x/\ell \qquad \omega_n^{*2} = n^2\pi^2T_e/M\ell^2 \; . \tag{38}$$

The modified frequencies from the perturbation solution are obtained by using (37) in (30)

$$b_n = W/2T_e \tag{39}$$

$$\omega_n^2 = (T_e + W/2)n^2\pi^2/M\ell^2 \; . \tag{40}$$

Although the formula for calculating b_n is lengthy, the result is rather simple. It should be noted that b_n is independent of n and the effect upon the frequencies is equivalent to replacing the non-uniform tension distribution by its mean value.

The perturbation coefficients for the mode shapes are now determined from (34) with $\delta(x)$ given by (37) and $\epsilon(x)$ equal to zero

$$a_m = - \frac{2\ mnW}{\pi^2(m^2 - n^2)T_e} \left[\frac{1}{(n - m)^2} + \frac{1}{(n + m)^2}\right] \tag{41}$$

where $m \neq n$, and m,n are both not odd and both not even. With this, the modified mode shapes can be expressed as

$$V_n(x) + \sum_{m \neq n} a_m V_m(x)$$

$$= \sin \frac{n\pi x}{\ell} - \frac{2W}{\pi^2 T_e} \sum_{m \neq n} \frac{mn}{(m^2 - n^2)} \left[\frac{1}{(n - m)^2} + \frac{1}{(n + m)^2}\right] \sin \frac{m\pi x}{\ell} . \tag{42}$$

For example, the shape for the fundamental mode is

$$\sin \frac{\pi x}{\ell} - \frac{W}{T_e} \left(0.1501 \sin \frac{2\pi x}{\ell} + 0.0082 \sin \frac{4\pi x}{\ell} + 0.0021 \sin \frac{6\pi x}{\ell} + \ldots\right) . \tag{43}$$

The exact gravity-gradient solutions for vibration frequencies and mode shapes previously obtained and the results from the perturbation analysis are, to a limited degree, complementary. For the mode shapes, the shifts in positions of maximum amplitude and crossing points, i.e. zeros, are in good agreement. The differences between numerical values for frequencies from the two solutions are small, particularly for small tension variations. This is

shown, for example, in Fig. 14 where a comparison is made for the fundamental frequency. The results for higher modes are similar.

VI. CONCLUSIONS

Exact solutions for the mode shapes and natural frequencies of completely flexible INPORT units have been determined. The major new improvement in the analysis of this problem is the proper assessment of the axial gravity gradient. This effect will be significant for INPORTs because of the large distance between supports and the relatively dense liquid metal which they convey. Results have been developed in parametric form for a range of values for pretension load and weight. It has been shown that strong asymmetric changes can occur in the mode shapes, particularly for large gravity gradients. Similarly, the results show that the numerical values of the natural frequencies for this problem can also be substantially different than the case in which the axial weight component is not included.

The exact solution was complemented by an approximate perturbation analysis. When the perturbation solution is used for computations, it should be limited to categories in which gradient effects are very small. Results for individual modes may only have small errors but larger errors can develop in forced response time histories which are based upon modal superposition. Thus for cases characterized by significant tension variations, it is emphasized that the exact solution should be used.

Accurate results for INPORT mode shapes are important for the LIBRA cavity design since these tubes are relatively close-packed and mechanical interference from motion must be avoided. Similarly, accurate values for the INPORT natural frequencies are important in the development of a design which

precludes resonance from synchronization with the repetition rate of the driver.

VII. REFERENCES

1. Engelstad, R.L. and Lovell, E.G., "Basic Theory for Three-Dimensional Motion of LIBRA INPORT Tubes," Fusion Power Associates Report FPA-84-2, October 1984.

2. McLachlan, N.W., Bessel Functions for Engineers, Oxford University Press, London, 1955, pg. 53.

Acknowledgement

Support for this work has been provided by the Kernforschungszentrum Karlsruhe, through a research agreement with Fusion Power Associates.

Table 1: NATURAL FREQUENCIES OF HEAVY TUBES

($\bar{\omega}_n$ n=1,...,1Ø.)

$\bar{T}$	1	2	3	4	5	6	7	8	9	1Ø
1.1ØØ	2.1Ø8	4.268	6.419	8.566	1Ø.712	12.858	15.ØØ3	17.148	19.293	21.438
1.2ØØ	2.4ØØ	4.834	7.261	9.686	12.111	14.535	16.959	19.382	21.8Ø6	24.229
1.3ØØ	2.634	5.294	7.948	1Ø.6Ø1	13.253	15.9Ø5	18.557	21.2Ø8	23.86Ø	26.511
1.4ØØ	2.838	5.697	8.551	11.4Ø5	14.257	17.11Ø	19.962	22.815	25.667	28.519
1.5ØØ	3.Ø23	6.Ø63	9.1ØØ	12.135	15.17Ø	18.2Ø5	21.24Ø	24.275	27.31Ø	3Ø.344
1.6ØØ	3.194	6.4Ø2	9.6Ø8	12.812	16.Ø16	19.22Ø	22.424	25.628	28.832	32.Ø36
1.7ØØ	3.354	6.72Ø	1Ø.Ø84	13.447	16.81Ø	2Ø.172	23.535	26.897	3Ø.26Ø	33.622
1.8ØØ	3.5Ø5	7.Ø21	1Ø.535	14.Ø48	17.561	21.Ø73	24.586	28.Ø98	31.611	35.123
1.9ØØ	3.649	7.3Ø8	1Ø.964	14.62Ø	18.276	21.931	25.587	29.242	32.898	36.553
2.ØØØ	3.786	7.582	11.375	15.167	18.96Ø	22.752	26.545	3Ø.337	34.129	37.922
2.1ØØ	3.919	7.845	11.77Ø	15.694	19.618	23.542	27.466	31.389	35.313	39.237
2.2ØØ	4.Ø46	8.Ø99	12.15Ø	16.2Ø1	2Ø.252	24.3Ø3	28.354	32.4Ø4	36.455	4Ø.5Ø5
2.3ØØ	4.169	8.344	12.518	16.692	2Ø.865	25.Ø39	29.212	33.385	37.559	41.732
2.4ØØ	4.288	8.582	12.875	17.167	21.459	25.752	3Ø.Ø44	34.336	38.628	42.92Ø
2.5ØØ	4.4Ø4	8.813	13.221	17.629	22.Ø37	26.444	3Ø.852	35.259	39.667	44.Ø74
2.6ØØ	4.516	9.Ø38	13.558	18.Ø78	22.598	27.118	31.638	36.158	4Ø.677	45.197
2.7ØØ	4.626	9.257	13.886	18.516	23.145	27.774	32.4Ø4	37.Ø33	41.662	46.291
2.8ØØ	4.733	9.47Ø	14.2Ø7	18.943	23.679	28.415	33.151	37.887	42.623	47.359
2.9ØØ	4.837	9.679	14.52Ø	19.36Ø	24.2ØØ	29.Ø41	33.881	38.721	43.561	48.4Ø1
3.ØØØ	4.94Ø	9.883	14.826	19.768	24.71Ø	29.652	34.595	39.537	44.479	49.421
3.1ØØ	5.Ø4Ø	1Ø.Ø83	15.125	2Ø.167	25.2Ø9	3Ø.251	35.294	4Ø.336	45.377	5Ø.419
3.2ØØ	5.138	1Ø.279	15.419	2Ø.559	25.699	3Ø.838	35.978	41.118	46.258	51.398
3.3ØØ	5.234	1Ø.47Ø	15.7Ø6	2Ø.942	26.178	31.414	36.65Ø	41.886	47.121	52.357
3.4ØØ	5.328	1Ø.659	15.989	21.319	26.649	31.979	37.3Ø9	42.639	47.969	53.299
3.5ØØ	5.42Ø	1Ø.844	16.266	21.689	27.111	32.534	37.956	43.379	48.8Ø1	54.223
3.6ØØ	5.511	11.Ø26	16.539	22.Ø52	27.566	33.Ø79	38.592	44.1Ø5	49.619	55.132
3.7ØØ	5.6Ø1	11.2Ø4	16.8Ø7	22.41Ø	28.Ø12	33.615	39.218	44.82Ø	5Ø.423	56.Ø26
3.8ØØ	5.689	11.38Ø	17.Ø71	22.761	28.452	34.143	39.833	45.524	51.214	56.9Ø5
3.9ØØ	5.775	11.553	17.331	23.1Ø8	28.885	34.662	4Ø.439	46.216	51.993	57.77Ø
4.ØØØ	5.861	11.724	17.586	23.449	29.311	35.174	41.Ø36	46.898	52.76Ø	58.623
4.1ØØ	5.945	11.892	17.838	23.785	29.731	35.678	41.624	47.57Ø	53.516	59.463
4.2ØØ	6.Ø28	12.Ø57	18.Ø87	24.116	3Ø.145	36.174	42.2Ø4	48.233	54.262	6Ø.291
4.3ØØ	6.1Ø9	12.221	18.332	24.443	3Ø.554	36.664	42.775	48.886	54.997	61.1Ø8
4.4ØØ	6.19Ø	12.382	18.574	24.765	3Ø.956	37.148	43.339	49.531	55.722	61.913
4.5ØØ	6.27Ø	12.541	18.812	25.Ø83	31.354	37.625	43.896	5Ø.167	56.438	62.7Ø8
4.6ØØ	6.348	12.698	19.Ø48	25.397	31.746	38.Ø96	44.445	5Ø.795	57.144	63.494
4.7ØØ	6.426	12.853	19.28Ø	25.7Ø7	32.134	38.561	44.988	51.415	57.842	64.269
4.8ØØ	6.5Ø2	13.ØØ6	19.51Ø	26.Ø14	32.517	39.Ø21	45.524	52.Ø28	58.531	65.Ø35
4.9ØØ	6.578	13.158	19.737	26.316	32.896	39.475	46.Ø54	52.633	59.213	65.792
5.ØØØ	6.653	13.3Ø7	19.962	26.616	33.27Ø	39.924	46.578	53.232	59.886	66.54Ø

Table 2: NORMALIZED MODE SHAPES

$\overline{T}$ = 1.100

x/l	1	2	3	4	5	6	7	8	9	10
0.000	0.000	0.000	0.000	0.000	0.000	0.000	0.000	0.000	0.000	0.000
0.025	0.041	0.071	0.101	0.132	0.156	0.192	0.228	0.244	0.263	0.287
0.050	0.082	0.143	0.202	0.261	0.304	0.370	0.432	0.451	0.475	0.505
0.075	0.125	0.215	0.300	0.382	0.436	0.516	0.583	0.585	0.588	0.591
0.100	0.168	0.286	0.393	0.489	0.540	0.612	0.657	0.617	0.571	0.516
0.125	0.211	0.356	0.478	0.576	0.607	0.648	0.640	0.537	0.421	0.292
0.150	0.255	0.423	0.552	0.637	0.631	0.616	0.531	0.354	0.168	-0.022
0.175	0.300	0.487	0.614	0.669	0.608	0.516	0.340	0.098	-0.132	-0.338
0.200	0.345	0.547	0.659	0.669	0.537	0.355	0.092	-0.184	-0.407	-0.558
0.225	0.390	0.602	0.687	0.634	0.421	0.149	-0.177	-0.436	-0.585	-0.608
0.250	0.435	0.650	0.696	0.565	0.267	-0.081	-0.425	-0.605	-0.614	-0.463
0.275	0.480	0.690	0.683	0.462	0.085	-0.308	-0.610	-0.647	-0.477	-0.159
0.300	0.525	0.723	0.648	0.331	-0.110	-0.502	-0.696	-0.548	-0.203	0.208
0.325	0.569	0.746	0.591	0.176	-0.300	-0.638	-0.663	-0.320	0.138	0.512
0.350	0.613	0.758	0.512	0.006	-0.469	-0.692	-0.508	-0.009	0.449	0.639
0.375	0.656	0.759	0.413	-0.170	-0.598	-0.653	-0.253	0.314	0.632	0.529
0.400	0.698	0.748	0.296	-0.342	-0.672	-0.518	0.060	0.569	0.620	0.210
0.425	0.738	0.725	0.163	-0.497	-0.679	-0.302	0.372	0.683	0.404	-0.205
0.450	0.777	0.688	0.018	-0.623	-0.614	-0.031	0.618	0.617	0.042	-0.549
0.475	0.815	0.637	-0.132	-0.710	-0.477	0.255	0.739	0.375	-0.347	-0.667
0.500	0.849	0.573	-0.283	-0.748	-0.280	0.510	0.698	0.013	-0.624	-0.489
0.525	0.882	0.494	-0.428	-0.729	-0.041	0.687	0.492	-0.367	-0.673	-0.074
0.550	0.911	0.403	-0.560	-0.650	0.214	0.747	0.156	-0.646	-0.455	0.393
0.575	0.938	0.298	-0.672	-0.513	0.452	0.669	-0.234	-0.723	-0.038	0.680
0.600	0.960	0.182	-0.755	-0.323	0.639	0.455	-0.580	-0.552	0.414	0.616
0.625	0.978	0.055	-0.802	-0.094	0.743	0.135	-0.779	-0.171	0.698	0.204
0.650	0.991	-0.079	-0.808	0.157	0.738	-0.231	-0.758	0.294	0.660	-0.348
0.675	0.999	-0.220	-0.767	0.406	0.613	-0.564	-0.498	0.666	0.284	-0.712
0.700	1.000	-0.362	-0.675	0.624	0.376	-0.777	-0.058	0.772	-0.265	-0.628
0.725	0.994	-0.504	-0.533	0.784	0.056	-0.801	0.428	0.533	-0.695	-0.103
0.750	0.980	-0.639	-0.344	0.856	-0.297	-0.604	0.786	0.020	-0.728	0.530
0.775	0.958	-0.762	-0.115	0.818	-0.613	-0.213	0.851	-0.538	-0.291	0.783
0.800	0.924	-0.868	0.142	0.659	-0.815	0.277	0.553	-0.835	0.380	0.389
0.825	0.879	-0.948	0.408	0.382	-0.835	0.710	-0.029	-0.650	0.814	-0.391
0.850	0.821	-0.996	0.659	0.014	-0.634	0.911	-0.646	-0.021	0.615	-0.841
0.875	0.746	-1.000	0.866	-0.394	-0.226	0.749	-0.958	0.681	-0.155	-0.413
0.900	0.653	-0.952	0.992	-0.765	0.302	0.221	-0.703	0.906	-0.844	0.549
0.925	0.538	-0.839	1.000	-1.000	0.783	-0.488	0.076	0.341	-0.665	0.869
0.950	0.396	-0.651	0.852	-0.993	1.000	-1.000	0.897	-0.644	0.373	-0.089
0.975	0.221	-0.375	0.521	-0.662	0.753	-0.888	1.000	-1.000	1.000	-1.000
1.000	0.000	0.000	0.000	0.000	0.000	0.000	0.000	0.000	0.000	0.000

Table 3: NORMALIZED MODE SHAPES

$\overline{T}$ = 2.000

x/l	1	2	3	4	5	6	7	8	9	10
0.000	0.000	0.000	0.000	0.000	0.000	0.000	0.000	0.000	0.000	0.000
0.025	0.062	0.119	0.176	0.231	0.288	0.339	0.401	0.439	0.489	0.545
0.050	0.125	0.238	0.346	0.447	0.546	0.627	0.718	0.757	0.808	0.856
0.075	0.188	0.353	0.504	0.634	0.746	0.816	0.879	0.860	0.837	0.789
0.100	0.251	0.464	0.644	0.775	0.861	0.871	0.844	0.713	0.557	0.365
0.125	0.313	0.567	0.757	0.860	0.876	0.779	0.615	0.351	0.066	-0.231
0.150	0.375	0.660	0.839	0.880	0.787	0.553	0.241	-0.120	-0.456	-0.727
0.175	0.436	0.742	0.886	0.831	0.601	0.228	-0.195	-0.561	-0.810	-0.888
0.200	0.496	0.811	0.894	0.717	0.339	-0.142	-0.590	-0.835	-0.854	-0.629
0.225	0.553	0.864	0.861	0.544	0.031	-0.491	-0.848	-0.850	-0.563	-0.063
0.250	0.609	0.900	0.789	0.324	-0.285	-0.756	-0.902	-0.596	-0.043	0.541
0.275	0.663	0.918	0.679	0.074	-0.569	-0.887	-0.733	-0.146	0.501	0.885
0.300	0.714	0.918	0.536	-0.185	-0.783	-0.854	-0.377	0.357	0.847	0.789
0.325	0.762	0.897	0.365	-0.432	-0.897	-0.660	0.080	0.750	0.845	0.290
0.350	0.806	0.857	0.174	-0.646	-0.893	-0.336	0.523	0.895	0.487	-0.366
0.375	0.847	0.798	-0.029	-0.807	-0.768	0.057	0.835	0.738	-0.085	-0.839
0.400	0.884	0.720	-0.233	-0.899	-0.535	0.445	0.929	0.323	-0.629	-0.872
0.425	0.916	0.625	-0.429	-0.912	-0.224	0.750	0.772	-0.212	-0.902	-0.435
0.450	0.943	0.513	-0.606	-0.841	0.124	0.907	0.400	-0.679	-0.776	0.246
0.475	0.966	0.388	-0.754	-0.691	0.459	0.879	-0.089	-0.907	-0.295	0.801
0.500	0.983	0.252	-0.864	-0.474	0.733	0.665	-0.561	-0.805	0.330	0.911
0.525	0.994	0.107	-0.929	-0.208	0.902	0.307	-0.878	-0.399	0.809	0.500
0.550	1.000	-0.043	-0.944	0.084	0.936	-0.125	-0.943	0.164	0.910	-0.209
0.575	0.999	-0.194	-0.907	0.371	0.827	-0.536	-0.727	0.674	0.570	-0.805
0.600	0.993	-0.343	-0.817	0.627	0.586	-0.833	-0.287	0.926	-0.056	-0.925
0.625	0.979	-0.486	-0.679	0.822	0.248	-0.946	0.250	0.812	-0.665	-0.479
0.650	0.959	-0.619	-0.497	0.935	-0.137	-0.840	0.717	0.365	-0.944	0.273
0.675	0.932	-0.737	-0.283	0.951	-0.507	-0.533	0.963	-0.241	-0.737	0.864
0.700	0.898	-0.838	-0.047	0.863	-0.797	-0.092	0.899	-0.756	-0.137	0.907
0.725	0.858	-0.917	0.197	0.678	-0.956	0.380	0.535	-0.955	0.548	0.354
0.750	0.810	-0.972	0.432	0.414	-0.951	0.766	-0.016	-0.739	0.944	-0.446
0.775	0.756	-1.000	0.645	0.096	-0.775	0.963	-0.573	-0.189	0.819	-0.955
0.800	0.695	-0.999	0.818	-0.239	-0.454	0.912	-0.938	0.458	0.224	-0.809
0.825	0.627	-0.967	0.940	-0.553	-0.043	0.618	-0.974	0.904	-0.512	-0.085
0.850	0.553	-0.906	1.000	-0.805	0.386	0.150	-0.653	0.930	-0.958	0.713
0.875	0.473	-0.814	0.990	-0.962	0.748	-0.370	-0.080	0.506	-0.832	1.000
0.900	0.388	-0.694	0.909	-1.000	0.970	-0.796	0.535	-0.177	-0.188	0.538
0.925	0.297	-0.548	0.758	-0.908	1.000	-1.000	0.954	-0.785	0.588	-0.348
0.950	0.202	-0.381	0.547	-0.692	0.823	-0.912	1.000	-1.000	1.000	-0.977
0.975	0.103	-0.196	0.288	-0.376	0.466	-0.545	0.638	-0.690	0.760	-0.833
1.000	0.000	0.000	0.000	0.000	0.000	0.000	0.000	0.000	0.000	0.000

Table 4: NORMALIZED MODE SHAPES

$\overline{T}$ = 3.000

x/l	1	2	3	4	5	6	7	8	9	10
0.000	0.000	0.000	0.000	0.000	0.000	0.000	0.000	0.000	0.000	0.000
0.025	0.068	0.133	0.196	0.262	0.325	0.380	0.446	0.501	0.547	0.606
0.050	0.137	0.264	0.385	0.505	0.610	0.694	0.785	0.846	0.877	0.917
0.075	0.205	0.390	0.558	0.708	0.820	0.882	0.931	0.920	0.854	0.775
0.100	0.273	0.510	0.705	0.854	0.926	0.909	0.845	0.694	0.481	0.243
0.125	0.340	0.620	0.821	0.930	0.911	0.765	0.543	0.238	-0.094	-0.416
0.150	0.405	0.717	0.898	0.927	0.776	0.475	0.100	-0.300	-0.634	-0.868
0.175	0.470	0.800	0.933	0.845	0.536	0.093	-0.372	-0.743	-0.913	-0.877
0.200	0.532	0.867	0.923	0.690	0.223	-0.311	-0.752	-0.938	-0.806	-0.431
0.225	0.592	0.915	0.867	0.473	-0.123	-0.658	-0.937	-0.816	-0.355	0.243
0.250	0.649	0.943	0.768	0.213	-0.456	-0.879	-0.877	-0.413	0.254	0.795
0.275	0.703	0.951	0.629	-0.069	-0.729	-0.929	-0.581	0.137	0.757	0.929
0.300	0.753	0.937	0.458	-0.347	-0.902	-0.794	-0.127	0.644	0.932	0.565
0.325	0.800	0.902	0.262	-0.596	-0.951	-0.498	0.366	0.928	0.696	-0.108
0.350	0.843	0.846	0.050	-0.793	-0.866	-0.099	0.763	0.884	0.148	-0.728
0.375	0.881	0.770	-0.166	-0.919	-0.656	0.324	0.953	0.523	-0.473	-0.951
0.400	0.914	0.675	-0.376	-0.961	-0.349	0.684	0.877	-0.031	-0.883	-0.648
0.425	0.942	0.564	-0.567	-0.914	0.011	0.905	0.553	-0.579	-0.892	0.022
0.450	0.965	0.437	-0.731	-0.780	0.373	0.937	0.069	-0.918	-0.488	0.685
0.475	0.983	0.300	-0.856	-0.569	0.683	0.770	-0.439	-0.918	0.148	0.962
0.500	0.994	0.153	-0.936	-0.302	0.894	0.436	-0.825	-0.572	0.720	0.686
0.525	1.000	0.002	-0.966	-0.003	0.971	0.005	-0.973	-0.006	0.954	0.008
0.550	1.000	-0.152	-0.942	0.299	0.901	-0.432	-0.834	0.568	0.731	-0.682
0.575	0.993	-0.303	-0.865	0.575	0.690	-0.778	-0.444	0.927	0.150	-0.972
0.600	0.980	-0.448	-0.738	0.796	0.370	-0.953	0.084	0.927	-0.510	-0.682
0.625	0.960	-0.583	-0.568	0.938	-0.012	-0.915	0.591	0.561	-0.923	0.024
0.650	0.934	-0.704	-0.363	0.986	-0.396	-0.668	0.921	-0.034	-0.878	0.722
0.675	0.902	-0.808	-0.134	0.932	-0.720	-0.264	0.968	-0.620	-0.388	0.980
0.700	0.863	-0.893	0.104	0.780	-0.931	0.206	0.710	-0.960	0.305	0.629
0.725	0.819	-0.954	0.339	0.544	-0.990	0.632	0.224	-0.907	0.847	-0.122
0.750	0.768	-0.990	0.557	0.247	-0.886	0.912	-0.339	-0.477	0.953	-0.803
0.775	0.711	-1.000	0.742	-0.080	-0.631	0.976	-0.798	0.159	0.557	-0.973
0.800	0.649	-0.982	0.884	-0.402	-0.267	0.803	-1.000	0.734	-0.140	-0.512
0.825	0.582	-0.937	0.972	-0.683	0.148	0.431	-0.871	0.999	-0.769	0.291
0.850	0.510	-0.865	1.000	-0.891	0.541	-0.053	-0.449	0.832	-0.985	0.909
0.875	0.433	-0.767	0.964	-1.000	0.844	-0.528	0.131	0.298	-0.661	0.921
0.900	0.353	-0.647	0.866	-0.996	1.000	-0.875	0.672	-0.375	0.035	0.308
0.925	0.268	-0.505	0.709	-0.877	0.978	-1.000	0.986	-0.886	0.718	-0.524
0.950	0.181	-0.348	0.504	-0.653	0.777	-0.866	0.956	-1.000	1.000	-1.000
0.975	0.091	-0.178	0.262	-0.349	0.431	-0.502	0.586	-0.654	0.708	-0.778
1.000	0.000	0.000	0.000	0.000	0.000	0.000	0.000	0.000	0.000	0.000

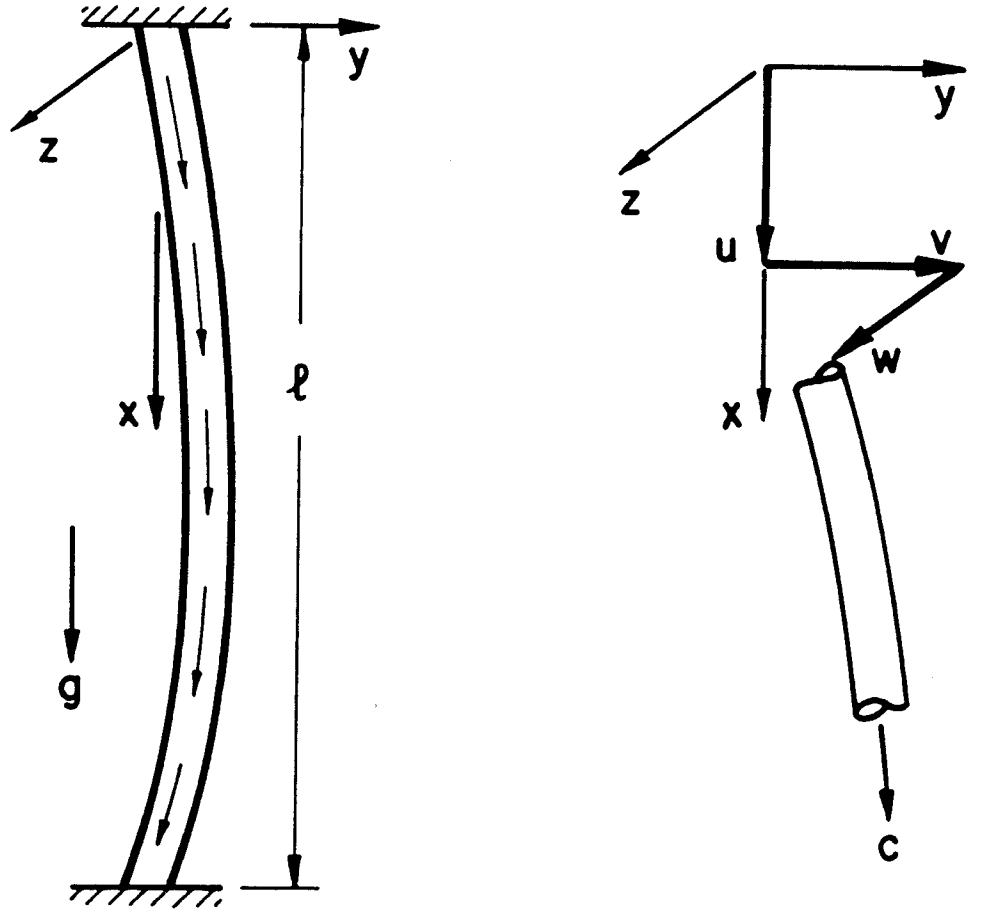

Fig. 1. Tube geometry and coordinate system.

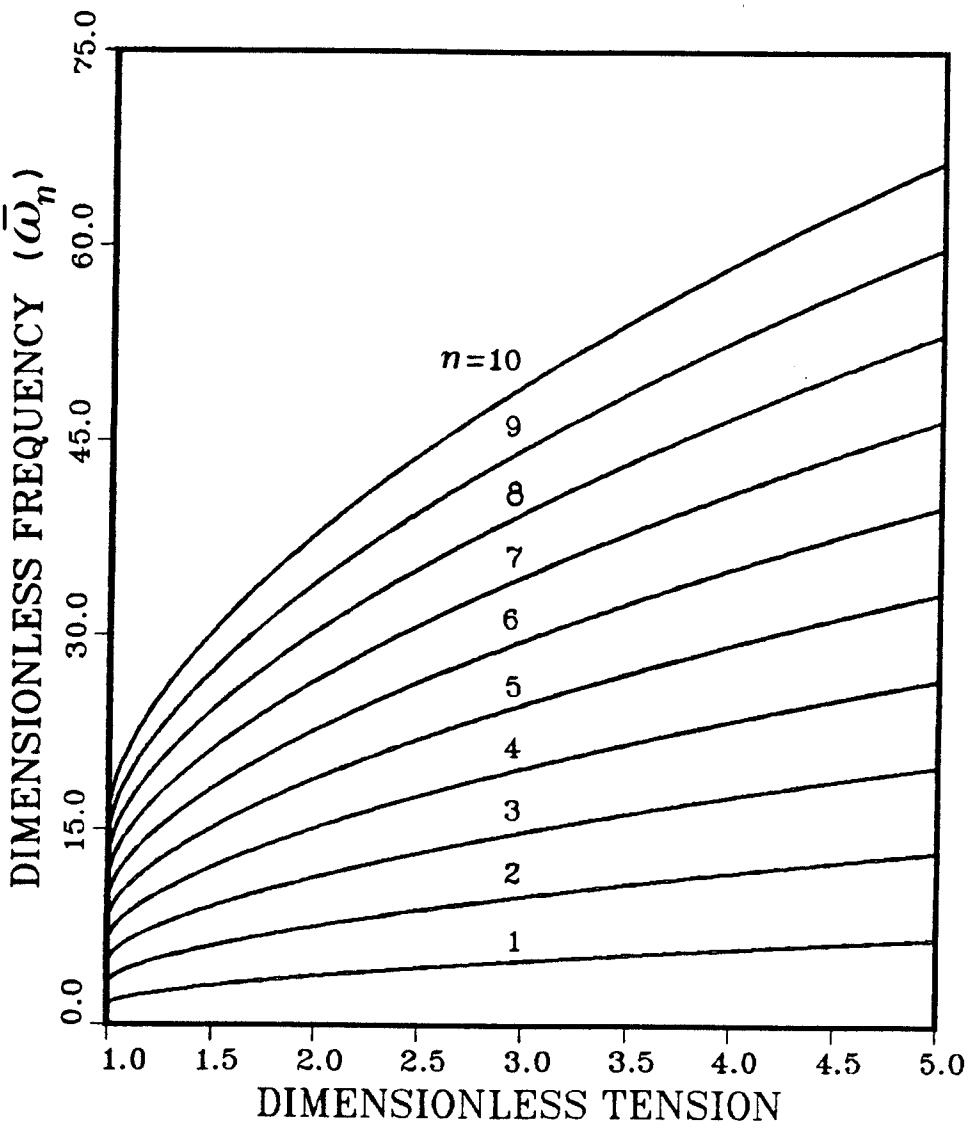

Fig. 2. Natural frequencies of heavy tubes.

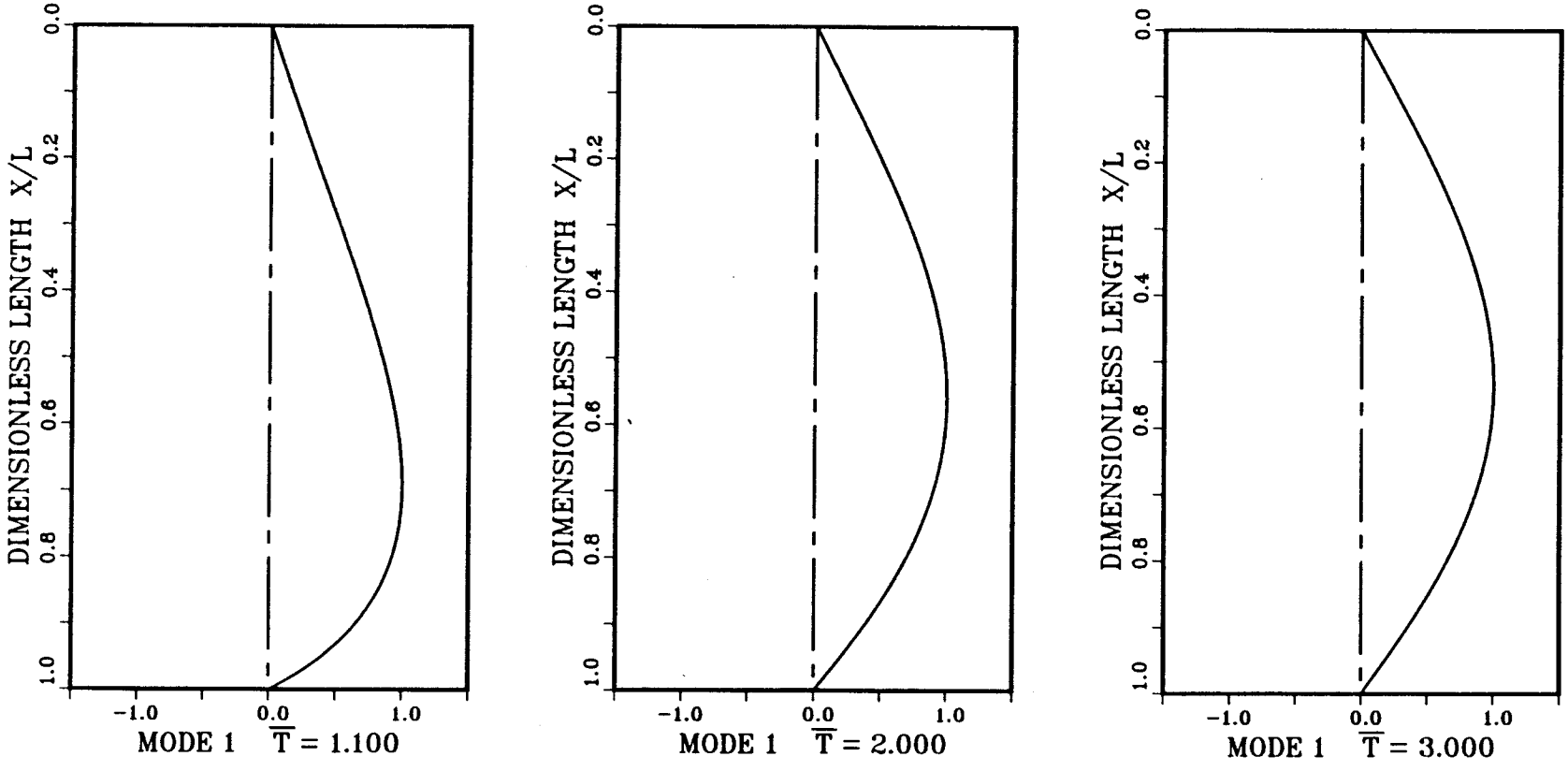

Fig. 3. Mode shape 1 for dimensionless tensions of 1.1, 2.0 and 3.0.

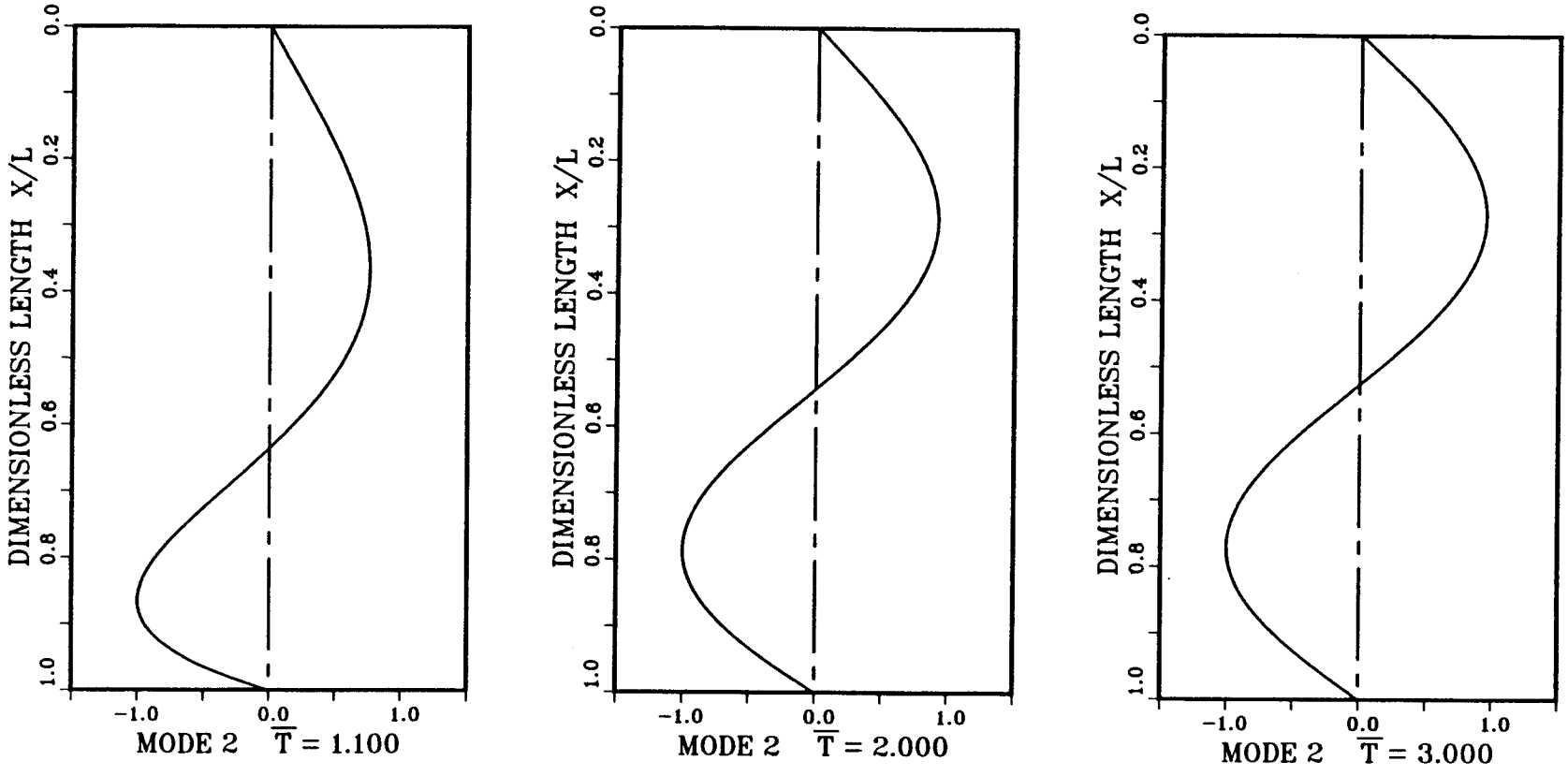

Fig. 4. Mode shape 2 for dimensionless tensions of 1.1, 2.0 and 3.0.

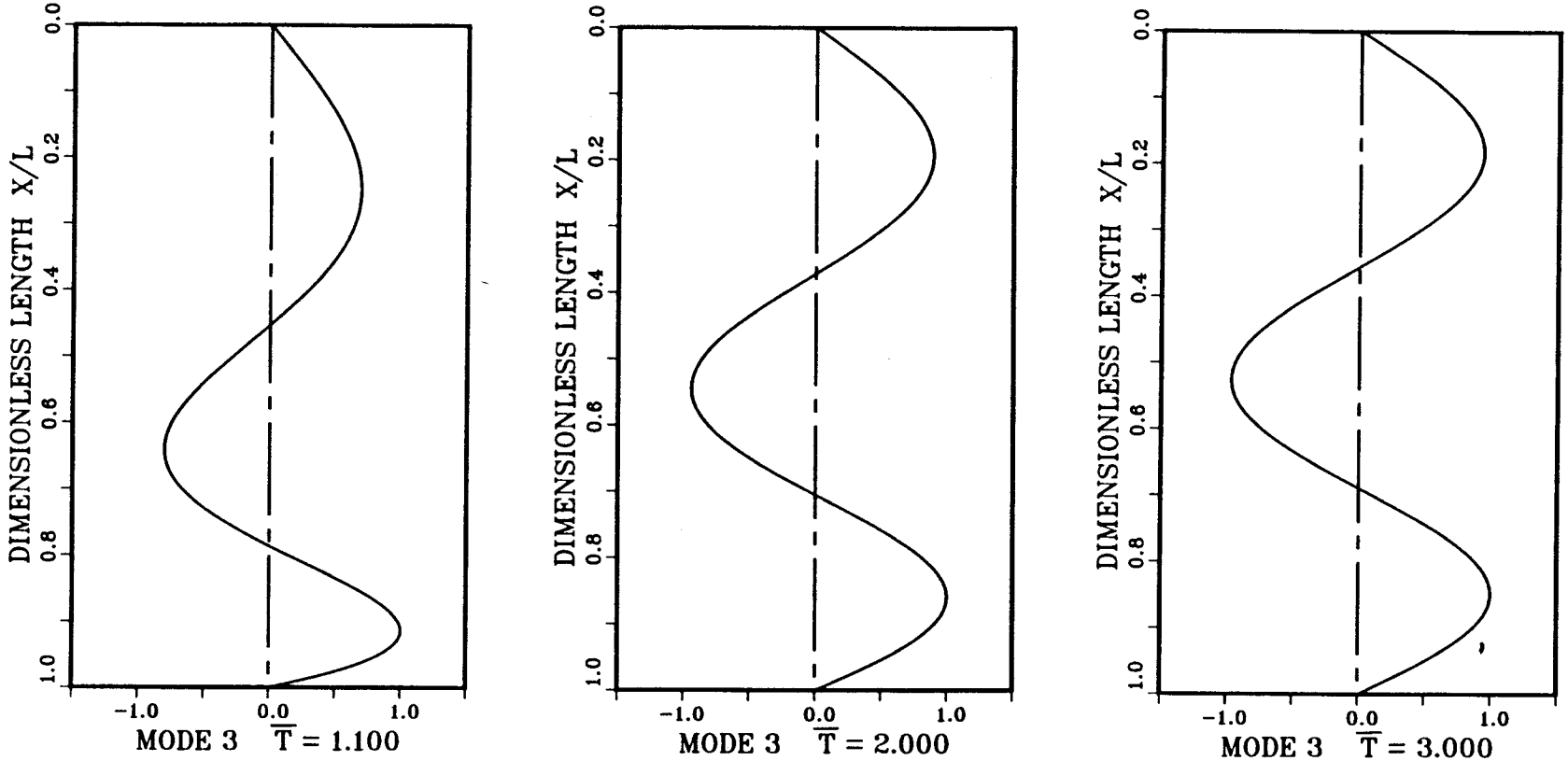

Fig. 5. Mode shape 3 for dimensionless tensions of 1.1, 2.0 and 3.0.

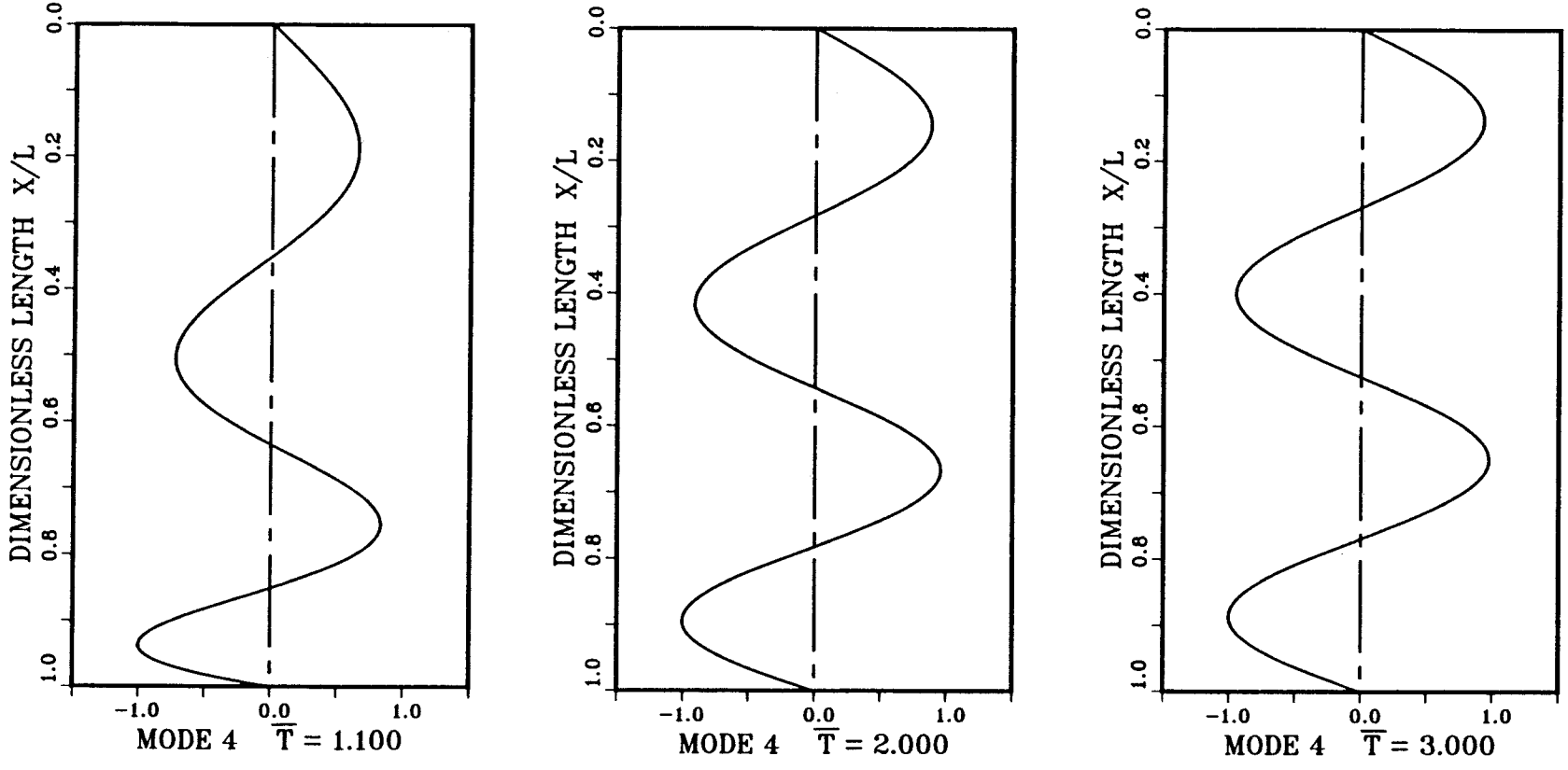

Fig. 6. Mode shape 4 for dimensionless tensions of 1.1, 2.0 and 3.0.

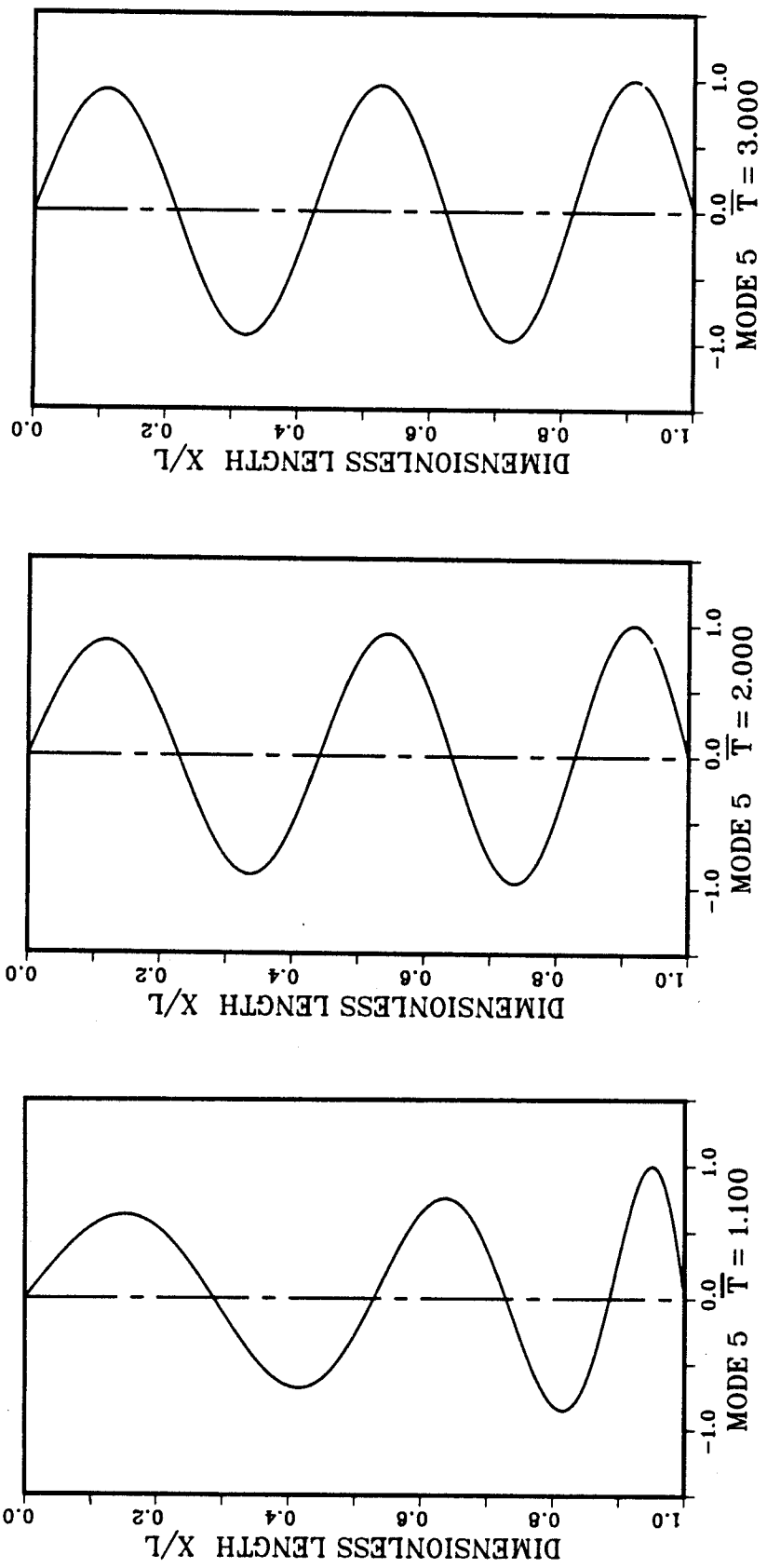

Fig. 7. Mode shape 5 for dimensionless tensions of 1.1, 2.0 and 3.0.

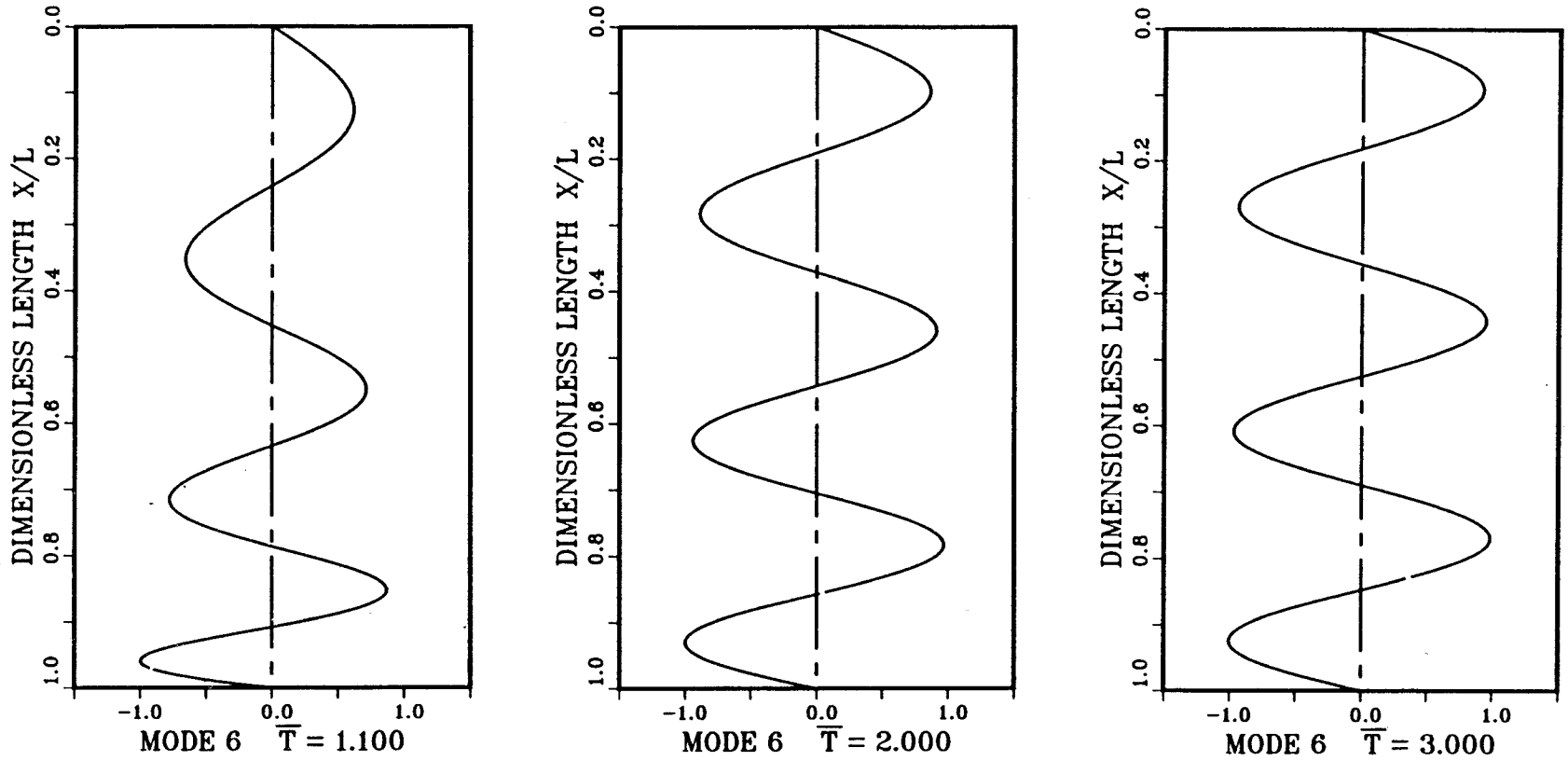

Fig. 8. Mode shape 6 for dimensionless tensions of 1.1, 2.0 and 3.0.

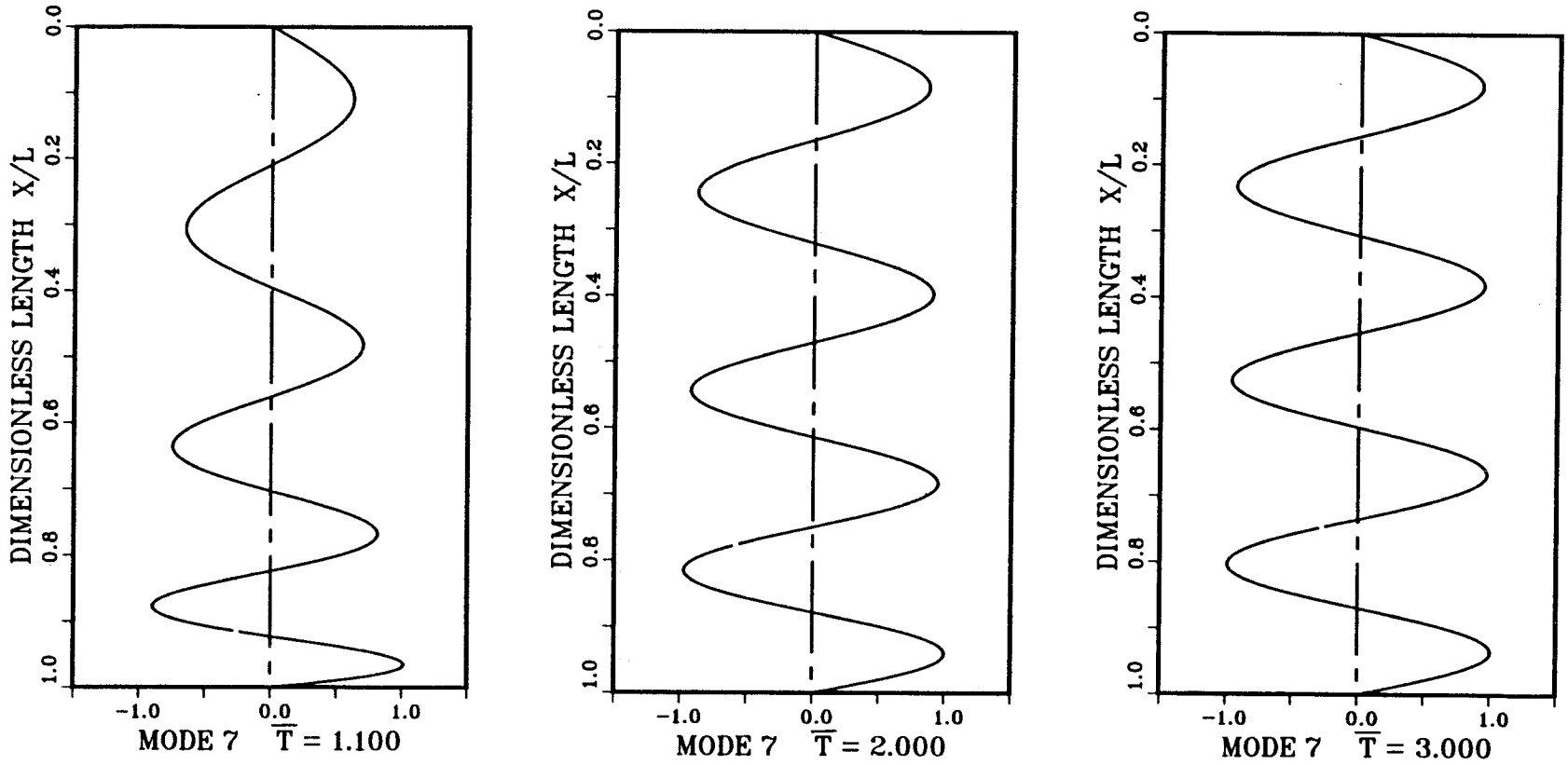

Fig. 9. Mode shape 7 for dimensionless tensions of 1.1, 2.0 and 3.0.

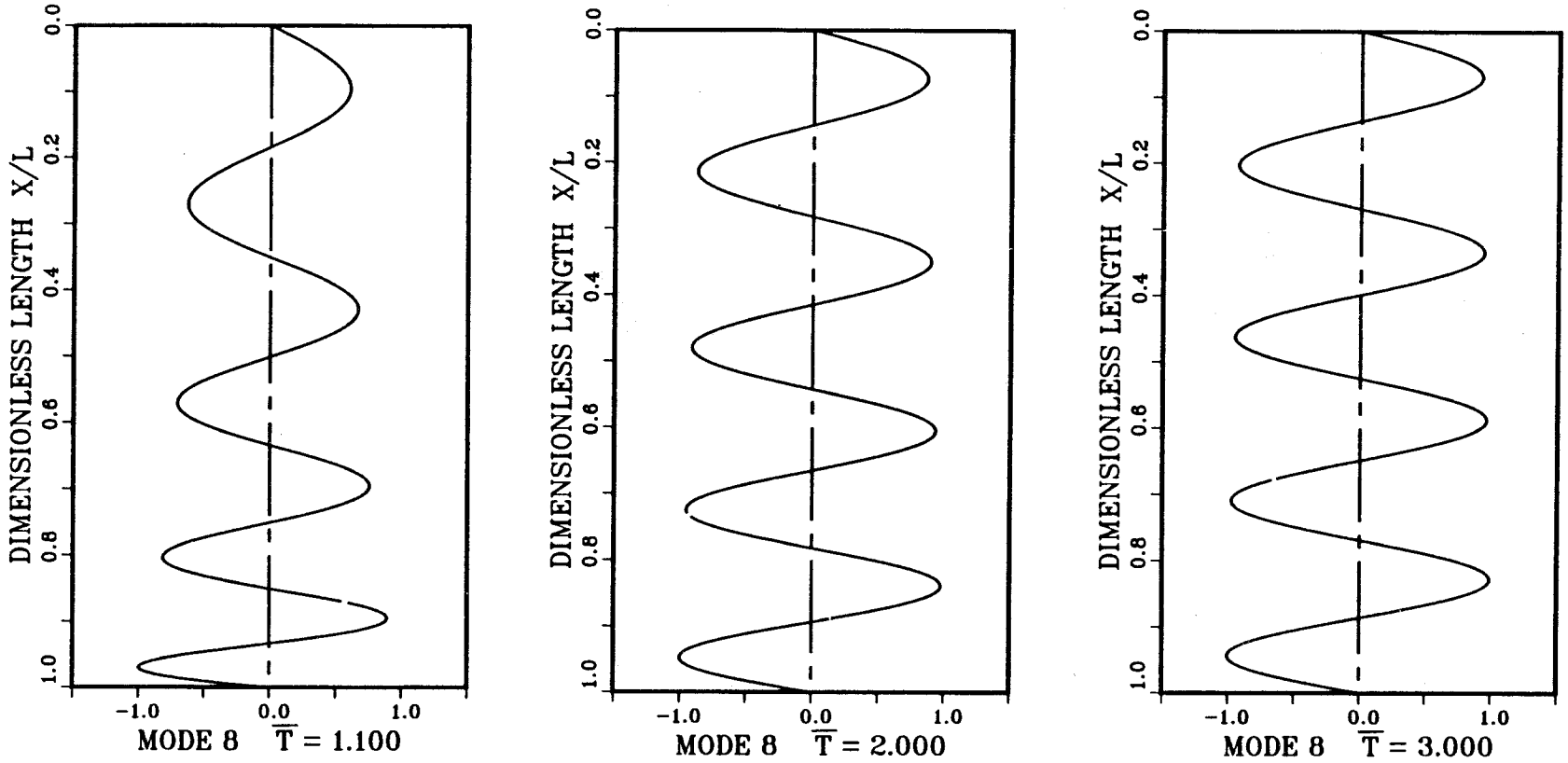

Fig. 10. Mode shape 8 for dimensionless tensions of 1.1, 2.0 and 3.0.

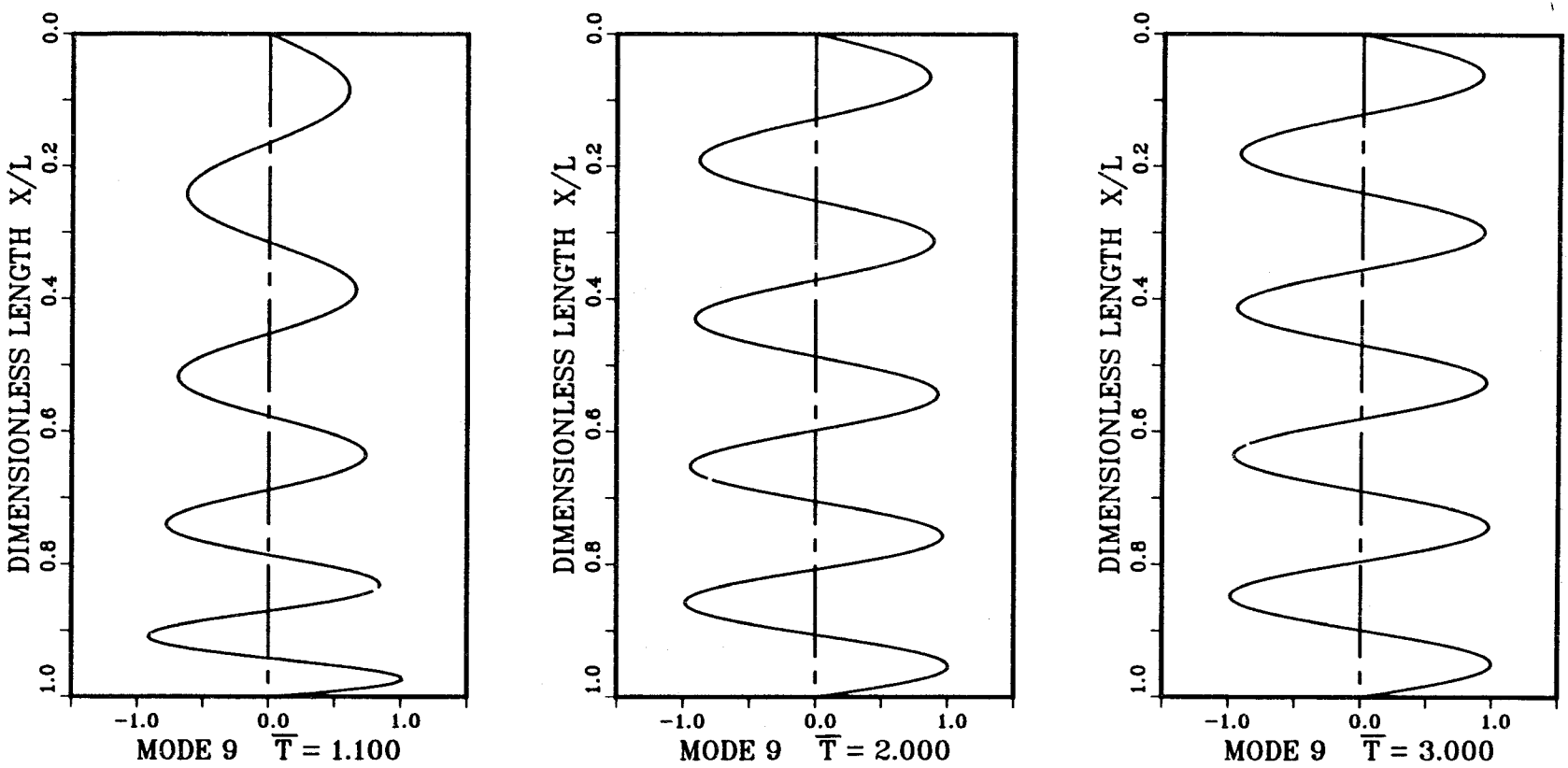

Fig. 11. Mode shape 9 for dimensionless tensions of 1.1, 2.0 and 3.0.

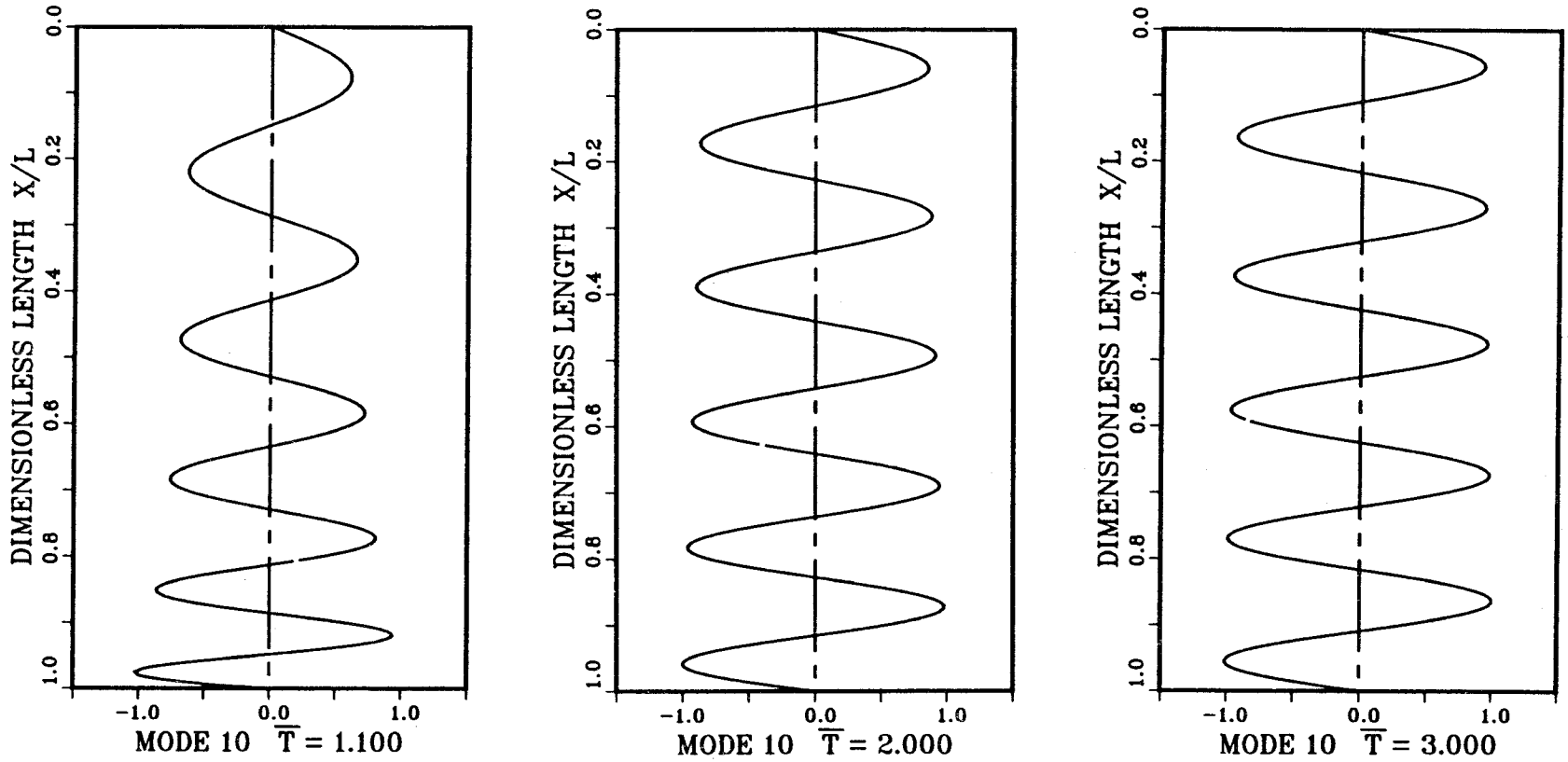

Fig. 12. Mode shape 10 for dimensionless tensions of 1.1, 2.0 and 3.0.

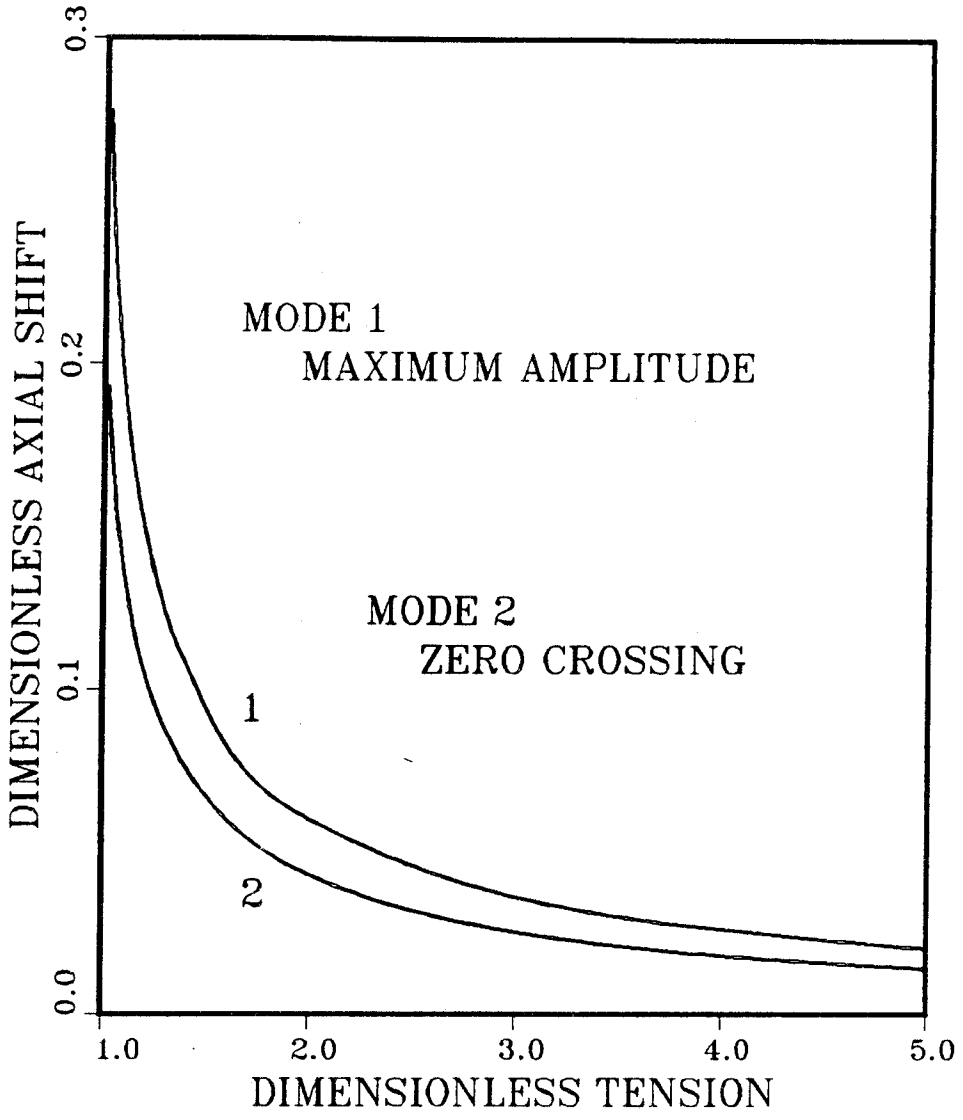

Fig. 13. Shifts in locations of maximum amplitude and zero crossings.

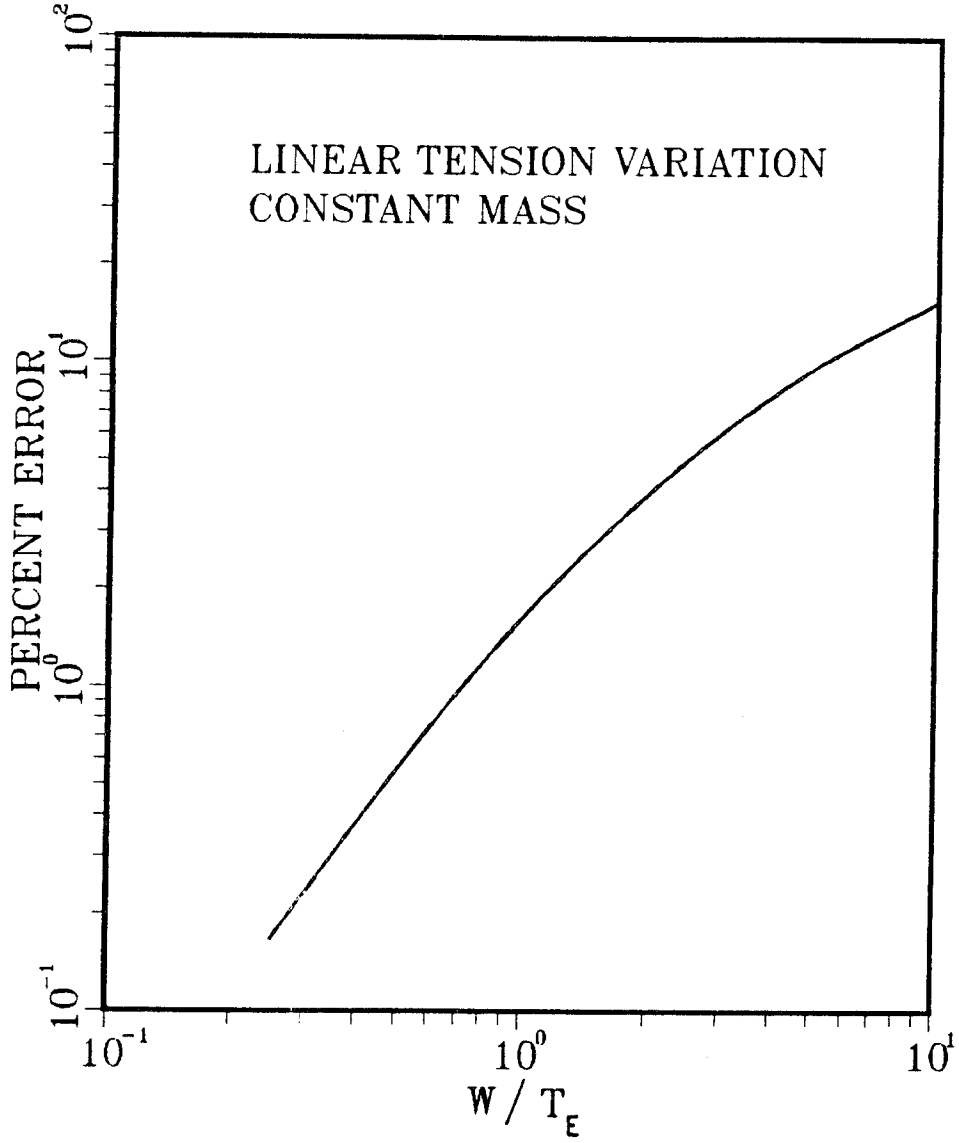

Fig. 14. Error in the fundamental frequency from the perturbation solution.